Available online at www.sciencedirect.com

ScienceDirect

Proceedings of the Combustion Institute 38 (2021) 1173–1180

Proceedings of the Combustion Institute

www.elsevier.com/locate/proci

# Pyrene dimerization in controlled temperature environment: An experimental study

M. Sirignano [a,*], C. Russo [b]

[a] *Dipartimento di Ingegneria Chimica, dei Materiali e della Produzione Industriale - Università degli Studi di Napoli "Federico II", P.le Tecchio 80, 80125, Napoli, Italy*

[b] *Istituto di Ricerche sulla Combustione – CNR – P.le V. Tecchio, 80 – 80125 Napoli, Italy*

Received 7 November 2019; accepted 7 June 2020

Available online 24 October 2020

**Abstract**

Nucleation step in soot formation can be defined as the transition from gas phase to condensed phase state at flame temperature. This aspect of particle formation in flame is the least understood despite of the great effort of the last decades. Most of the models and of the experimental setups are not able to isolate the single step of nucleation. The formation of the first particles or species in condensed phase is studied in combustion environments in which many other processes – namely PAH growth from other small hydrocarbons and oxidation – are taking place. A tubular flow reactor working in the temperature range of 800–1100 K with a stream containing pure PAH – pyrene in the current work - was used to isolate the pathways leading from gas to condensed phase. To avoid the formation of smaller compounds from the pyrene pyrolysis, temperature was kept lower than 1100 K allowing a residence time long enough to favour mass growth. DMA measurements at the exit of the reactor showed the presence of particles. Particle formation was found to be sensitive to the temperature. In particular, the formation rate was higher at the higher temperature, suggesting the intervention of some chemical-driven pathway for the formation of the first condensed phase species. The gas and the particles exiting the reactor were trapped in ethanol and analyzed by UV-Visible and fluorescence spectroscopy, and size exclusion chromatography (SEC). The formed particles have lost molecular spectral features and have a molecular weight (MW) >= 400: these characteristics allow to consider them the smallest species in condensed phase. Their MW evaluated by SEC and the analysis of their absorption spectra hinted to the predominance of oligomers formation, from dimers to tetramers, being trimers the most favored and stable species in the investigated conditions.
© 2020 The Combustion Institute. Published by Elsevier Inc. All rights reserved.

*Keywords:* Pyrene; Nucleation; Particle inception; Condensed phase nanostructures; Soot

## 1. Introduction

Soot has been studied extensively in the last decades, delving into its features, mechanisms of formation to the extent of its application in nanotechnology [1,2]. Aspects of soot formation such

* Corresponding author.
*E-mail address:* mariano.sirignano@unina.it (M. Sirignano).

https://doi.org/10.1016/j.proci.2020.06.367
1540-7489 © 2020 The Combustion Institute. Published by Elsevier Inc. All rights reserved.

as the surface growth, coagulation and aggregation are well-known and accepted in literature and well treated by current soot models. Similarly, combustion kinetics of gas phase high molecular weight compounds, from benzene to pyrene, have been also largely studied, reaching a consensus on some reaction pathways and the kinetics governing them [2]. The missing step remains the transition from the largest compound still belonging to gas phase and the first compound no longer possible to be considered in gas phase [3,4]. The limit between these entities has been found to be very subtle and thus from here the latter will be referred to as the smallest species in condensed phase.

The problem has been tackled experimentally by using state-of-the-art techniques, pushing to the limit of their possibilities. Optical techniques were used to detect the smallest particles by absorption and laser induced fluorescence [4–7] and - in particular conditions - incandescence [8]. The use of ex situ techniques has been also widely exploited. The high-resolution transmission microscopy (HR-TEM) has furnished interesting insights on small particles but there is still no result about the detection with this technique of the smallest species in condensed phase [9]. Atomic force microscopy (AFM) has been used to give information on PAH constituents of the smallest species deposited from flames [10,11]. Differential mobility analysis (DMA) has been used to track the evolution of particle size distribution (PSD), pushing the detection limit down to 1 nm [12,13]. Finally, also laser-ionization mass spectrometry has been used furnishing the evidence of the presence of compounds as small as dimers, trimers of PAH [14].

Models have taken advantage through years of the increasing knowledge derived from experimental findings, moving towards more sophisticated ways of treating the different processes of particle formation. Generally, models tackle nucleation process moving from treating the single specific compounds in gas phase with appropriate kinetics to the use of particle models based on lumped species and kinetics also decoupled from gas phase. Many models have been adopted pyrene dimerization as the only nucleation step to initiate particle formation. The dimerization was initially considered having unitary efficiency, and successively having a much lower efficiency. Still nowadays many models adopt a high sticking efficiency for pyrene, despite of the fact that molecular dynamic (MD) and other quantum mechanics (QM) approaches [15–20] strongly suggest that this process is not feasible, although a definitive consensus is not reached. MD and QM simulations have been used to tackle the single step of the nucleation, i.e. effectively proving that pyrene was indeed able to dimerize at temperature typical of combustion systems (usually $T > 1500$ K) [21]. Despite of the great work, there is no consensus whether gas-phase PAH not larger than pyrene are effectively able to stick and survive in combustion environment. Differing from the pure PAH-sticking approach, the possibility to adopt a chemical pathway to produce the smallest species in condensed phase has also fascinated the scientists from the beginning. The chemical growth of PAH, eventually including 5-membered rings, has been thought to be leading up to fullerenes or a fullerene-like structures which would have been the starting point or the smallest species in condensed phase. This pathway has also been proved to be not feasible, unless in particular combustion conditions in which fullerene formation is favored [2]. Finally, the possibility to link several PAH by aliphatic bridges has also been explored [22]. The mechanism has been developed in the early 2000's and it has been adopted together with and in alternative to the PAH-sticking approach. Very recently the possibility to obtain the smallest species in condensed phase starting from PAH radicals and using this peculiarity to establish a strong interaction between PAH, stronger than the Van der Waals interaction driving the classical sticking mechanism, was also explored [23,24]. On the nature of this interaction studies are still ongoing.

Developing experiments that can support the ongoing theoretical studies is at the basic of this work. Isolating the nucleation step from the experimental point of view is quite difficult. In combustion environment nucleation is competing with all the other pathways including growth and oxidation. To isolate the nucleation step, in this work pyrene has been chosen as a model PAH to be studied in a controlled environment, constituted of a tubular flow reactor at controlled temperature. Most of the works carried out in this reactor for studying soot have been focused on ethylene or acetylene. Other studies using benzene [25], toluene [26,27], the addition of C2 species to C6 aromatics [28], ethylbenzene, and ethyl alcohol [29,30] have been reported. A recent study on aromatics was conducted by using benzene and PAH such as pyrene and coronene [31]. The study is of great relevance for understanding the mechanism of nucleation. However, the study has been conducted always in presence of benzene and at very high temperature (1400-1650 K). At this temperature and considering the amount of benzene present in the reactor (1400 ppm) the formation of smaller species from pyrolysis was considerable. Similarly Sarofim et al. [32] conducted a study on anthracene and pyrene at much higher temperature (1200-1500 K) also hypothesizing the role of aryl-aryl recombination, however large amounts of decomposition products were present and experimental evidences could not be considered definitive on this point.

Hence from these previous works it is not possible to distinguish whether PAH are effectively forming new particles or are just adding/condensing onto existing ones derived from pyrolysis products. Nucleation from large PAH - pyrene

Table 1
Investigated operative conditions.

| $N_2$ [Nl/min] | Ar [Nl/min] | $T_{Pyrene}$ [K] | Measured $C_{Pyrene}$ [ppm] | T reactor [K] | Residence time [s] |
|---|---|---|---|---|---|
| 25 | 0.60 | 403 | 5.2 | 800 | 0.113 |
| 25 | 0.60 | 403 | 5.2 | 900 | 0.101 |
| 25 | 0.60 | 403 | 5.2 | 1000 | 0.091 |
| 25 | 0.60 | 403 | 5.2 | 1100 | 0.082 |
| 25 | 0.60 | 453 | 47 | 1000 | 0.091 |
| 25 | 0.60 | 453 | 47 | 1100 | 0.082 |

in this work – is studied at much lower temperature, namely up to 1100 K, and much lower concentration (tens of ppm). Overall, the chosen conditions, together with the possibility to feed pure pyrene into the reactor, help to shed light on the first step of formation of the smallest species in condensed phase. The aim of this work is to assess whether it is possible to form condensed phase nanostructures in the chosen conditions, whether these condensed phase nanostructures are similar to those found in a combustion environment and finally to assess the role of temperature in the inception process.

## 2. Experimental set-up

The experimental apparatus built to study the particle inception from PAH as pyrene consists of a tubular flow reactor, a quartz saturator, and two pre-heaters. A schematic of the experimental set up is reported in the supplemental (Fig. S1). Here a detailed description is furnished.

The quartz saturator is constituted of a 250 ml flask heated and insulated in which has been introduced milled pyrene crystals. Pyrene was introduced into the tubular flow reactor by sublimating the solid crystals using an argon stream set at 0.60 Nl/min and preheated at the same temperature of quartz saturator. The saturator temperature was controlled with a precision of 0.5 K. A second pre-heater heated up a flow rate of nitrogen, used as main carrier gas of pyrene. Nitrogen and argon streams were mixed at the exit of the quartz saturator, and then sent to the inlet of the reactor. The above procedure allowed obtaining a stream containing pyrene with a specific concentration. Pyrene concentration at the entrance of the reactor, i.e. after the mixing with the heated nitrogen stream, was measured by sampling 1 l/min from the main stream and bubbling it in a two-stage bubbler filled with ethanol. Concentrations of pyrene present in the mainstream and dissolved in ethanol solutions were determined by a calibration curve obtained using the Lambert-Beer relationship between concentration and UV-Visible (UV–Vis) absorbance derived from a series of standard solutions of pyrene in ethanol.

High purity nitrogen was supplied by using Brooks mass flow controllers. At the exit of the reactor a DMA was used to analyze the PSD functions. The nitrogen/argon/pyrene mixture flowed through a tubular flow reactor, similar to a plug tubular flow reactor (PFR). Cold nitrogen was also used in a secondary flow rate in order to prevent a high temperature at DMA inlet.

The reactor was constituted of a 7 mm ID and 3.6 m long quartz tube, because this material is inert and resistant at the chosen working temperatures. Temperature was controlled along all the branches of the PFR and kept constant within ±25 K. The PSD functions were measured by nano-DMA, Vienna type (model 3085) equipped with a bipolar Advanced Aerosol Neutralizer uses a low-energy (<9.5 keV) soft X-ray source. In the configuration adopted the size range was 0.6–28 nm. The classified particles were counted by a Faraday cup electrometer (FCE).

The nitrogen flow rate used as carrier gas was fed to the PFR with a flow rate of 25 Nl/min. In these conditions Reynolds number was above laminar transitions and the residence time was in the range of 0.113–0.082 s inside the 3.6-meter tubular flow reactor at the controlled temperature range of 800 – 1100 K. The operating conditions chosen to conduct the investigations are summarized in Table 1. Finally, a nitrogen flow rate of 3.5 Nl/min was used to dilute and to cool down the stream entering into the DMA (safety limit 50 °C). The flow rate of nitrogen dilution was chosen to optimize the signal-to-noise ratio determined by the electrometer sensitivity (10 fA); on the other side the concentration in the sampling line cannot be too high due to coagulation issues.

Off-line measurements were also carried out. Particles exiting from the reactor were sampled by a two-stage bubbler positioned ahead the DMA. The bubbler was filled with 100 ml of ethanol in order to trap both pyrene and larger species, if any, exiting from the reactor. Reactor particles features have been compared with flame-formed particles, sampled at 15 mm height above the burner in an ethylene/air flame ($\varphi = 2.01$) and suspended in ethanol. All the solutions before being analysed were filtered on an Anotop filter <20 nm (Whatman) to remove any impurities. The solutions were then analyzed with UV-Vis and fluorescence spectroscopy. UV-Vis spectra of sample dissolved in ethanol were measured in the 190–1100 nm wavelength range

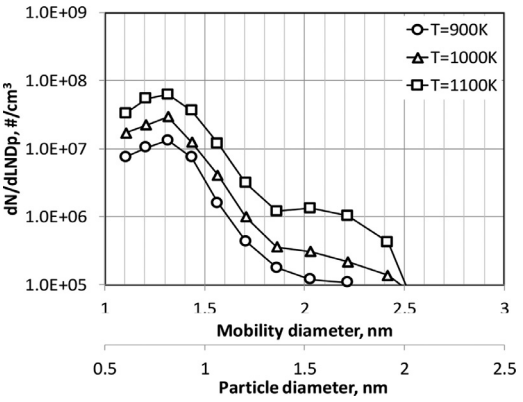


Fig. 1. PSD measured at the exit of the reactor heated up at different temperatures (see legend), with fixed temperature of the quartz saturator ($T_{Pyrene}$ 403 K.– 5 ppm).

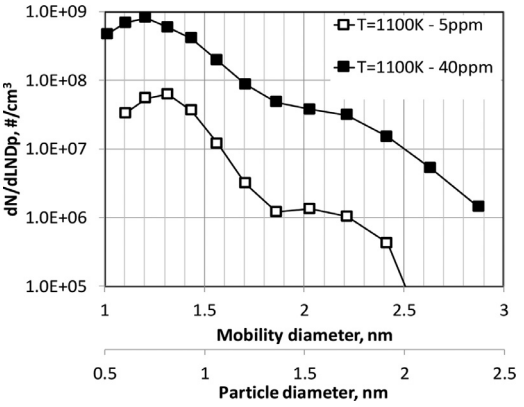


Fig. 2. PSD measured at the exit of the reactor for a fixed temperature (1100 K), with different pyrene concentrations.

on an HP 8453 Diode Array spectrophotometer using 1 cm quartz cuvettes. Fluorescence spectra were acquired on a PerkinElmer LS-50 spectrofluorimeter using a xenon discharge lamp as excitation light source [33]. Samples were then slowly dried and dissolved in N-methyl pyrrolidone (NMP). It is worth to underline that the UV-Vis spectra of the samples measured before and after the drying and dissolution kept the same shape demonstrating that this procedure did not modify the sample structure in terms of agglomeration. Moreover, if weak bonds be possibly formed they would be disrupted by dissolution in NMP and sonication. Size exclusion chromatography (SEC) was carried out on HP1050 high pressure liquid chromatograph (HPLC) using NMP as eluent for evaluating the molecular weight (MW) distribution of the sample. The HPLC was equipped with a diode array detector (DAD) to measure the on-line UV–Vis absorbance of the eluting compounds from 250 nm up to 600 nm. A highly cross-linked "individual-pore" column [34] was used to analyze the sample in the MW range from 100 u to 1E5 u. The SEC calibration curve used for the MW evaluation was obtained using polystyrene and PAH standards.

## 3. Results and discussion

PSD measured by DMA at the exit of the reactor heated up at different temperatures – from 900 K up to 1100 K – are reported in Fig. 1 for a fixed temperature (403 K) of quartz saturator containing pyrene. At 800 K there was no evidence of particles formed. For a temperature of the reactor of 900 K particles start being detected in small amounts. When the temperature reaches 1000 K and then 1100 K the particles are formed already with the smallest amount of pyrene into the reactor. It is worth to note that the PSD are plotted against the mobility diameter which is the axial coordinate used by the instrument. As secondary X-axis a particle diameter is also reported. This is obtained by the mobility diameter by subtracting 0.5 nm [35]. Although this procedure has been used in the past, particle diameter axis is here reported just for a quick comparison with other literature data. An error on the exact evaluation of particle diameter by using the classical relation can be induced considering the nature of incipient condensed phase of the detected species. It is beyond the scope of this work to assess the relation between the particle diameter and the mobility diameter for these particles.

In order to better evidence the role of pyrene concentration at highest reactor temperature (1100 K) the results have been reported in Fig. 2 for different temperatures of quartz saturator containing pyrene. It is possible to observe how the system is sensitive to the pyrene concentration. As the pyrene concentration increases the number of particles formed increases. Also, there is no evidence of particles larger than 3 nm indicating that the process involved is just the nucleation, or that at least the growth towards larger particles is negligible or not effective. Overall the positive effect of temperature suggests that a chemical-driven inception is more likely to be effective in the investigated conditions. In fact, according to the classical theory [36] as the temperature increases the sticking efficiency should decrease. Thus, an increase in the inception rate has to be linked with other mechanisms which involve an energetic barrier, such as the formation and successive interaction of radicals.

After assessing that in certain reactor conditions some particles are formed, it is important to verify if these particles are similar to those formed in a flame at much higher temperature and different environment. Further investigations of the chemico-physical nature of these incipient nanostructures

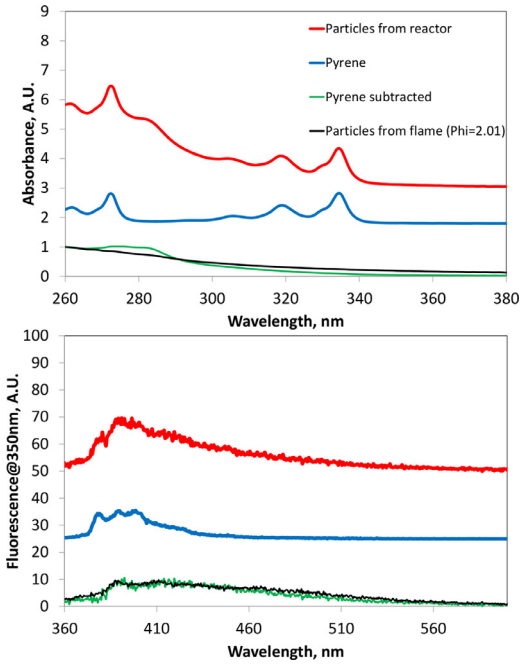


Fig. 3. UV-Vis (upper part) and fluorescence spectra excited at 350 nm (lower part) of reactor particles, pyrene and particles from ethylene/air flame ($\varphi = 2.01$) dissolved in ethanol. The spectra obtained as difference between the spectra of reactor particles and pyrene are also reported.

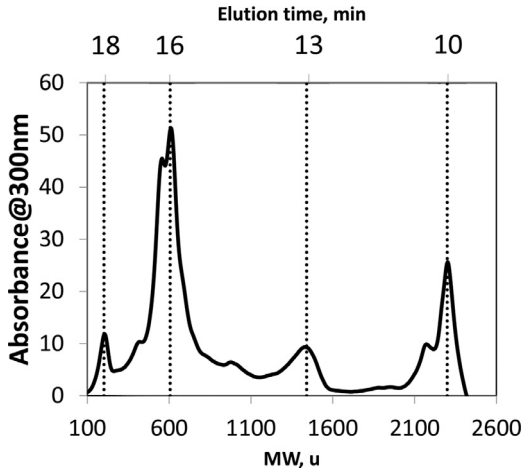


Fig. 4. SEC chromatogram of the reactor particles for a fixed temperature of the reactor of 1100 K and a $T_{Pyrene}$ of 403 K. Dotted lines indicate the points where UV-Vis spectra have been used for reconstructing the bulk UV spectra (see Fig. 5).

by means of off-line batch analysis have been performed. The stream at the exit of the reactor was bubbled into ethanol to trap the particles. Ethanol has been chosen since it is very prone to dissolve organic matter and easy to evaporate to obtain higher concentration mandatory for further analyses. First of all, samples have been analyzed by UV-Vis spectroscopy and the spectrum obtained for the highest reactor temperature and pyrene concentration is reported in Fig. 3 (top panel) in comparison with the spectrum of a typical carbon particulate matter sampled at 15 mm height above the burner in an ethylene/air flame ($\varphi = 2.01$), and suspended in ethanol. This flame condition is used here as reference, because it is characterized by a monomodal PSD peaked at 1-3 nm [4,12] similar to those reported at the exit of the reactor (Fig. 1 and Fig. 2). It can be noted that the spectra are quite similar. The sample collected at the exit of the reactor still contains pyrene as it appears from the sharp spectral peaks detected. Overall looking at the spectrum of the reactor sample obtained by subtracting the pyrene contribution it appears evident that both reactor and flame samples exhibit an unstructured absorption spectrum typical of condensed phases [34].

The reactor particles were also analyzed by fluorescence spectroscopy. The emission spectrum obtained with an excitation wavelength of 350 nm is reported in Fig. 3 (bottom panel) and compared with the spectra of pyrene dissolved in ethanol and of the particles collected from flame. The emission spectra show that particles at the exit of the reactor have lost the fine structure featuring pyrene emission moving toward a broader and unstructured spectrum. The spectrum obtained by difference between the spectrum of the reactor particles and pyrene one matches quite satisfactorily with that measured for the ethylene flame.

The chromatogram measured by SEC analysis of the sample collected at a fixed temperature of the reactor of 1100 K and at temperature of 403 K of quartz saturator is reported in Fig. 4. A detection wavelength of 300 nm was chosen to avoid the interference of the solvent (NMP) absorbing up to 260 nm and to have a spectral intensity enough high to get a clearer and reproducible chromatogram. Indeed, as will be shown in the following (Fig. 5), all the detected species present very low UV-Vis signals above 340 nm. The first peak, obviously due to pyrene, is noted around 200 u whereas it is remarkable that there is no evidence of compounds smaller than pyrene ($<$200 u). The absence of species up to 300 u different from pyrene was also confirmed by GC-MS analysis of the reactor sample. From 300 to 800 u, an intense and indented absorption peak is observed with a maximum around 600 u and presenting a small shoulder at about 400 u. The presence of other peaks at higher molecular weights $>$1000 u is noticeable.

More information on the nature of these species is given by the UV-Vis spectra measured on the apex of the main SEC peaks located around 200,

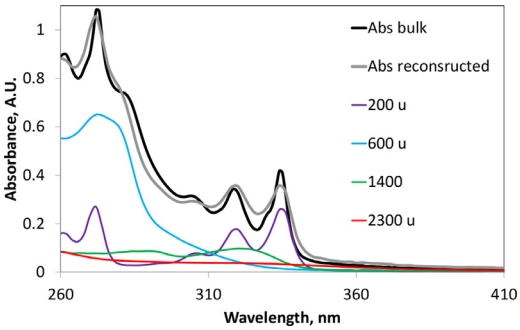


Fig. 5. Reconstruction of the UV-Vis spectrum of particles exiting from the reactor as sum of the UV-Vis spectra measured on the apex of the main MW-segregated fraction of SEC chromatogram of the sample collected at the exit of reactor for a fixed temperature of the reactor of 1100 K and $T_{Pyrene}$ of 403 K.

600, 1400 and 2300 u, reported in Fig. S2 and compared in Fig. 5 with the absorbance spectrum of the reactor sample measured in cuvette. The spectra measured on the apex of the peaks in Fig. 5 have been reported taking into account for their contribution to the whole spectrum. The fine structure of the spectrum recorded at 200 u confirms the attribution to pyrene. The species at 600 u present a broad absorption with a bump at 270 nm whereas the 1400 u spectrum presents two bumps of equal intensity in the UV at 280 nm and 320 nm. Finally, the 2300 u spectrum extending up to 450 nm, is characterized by a broad shape with a shoulder at 320 nm. The attribution of peaks above pyrene to specific class of species is not straightforward. On the basis of the MW it can be speculated that they are due to pyrene oligomers. The shoulder at 400 u and the high peak at 600 u could be attributed to dimers and trimers, respectively, on the basis of their MW. Higher oligomers like hexamers and dodecamers should be attributed to the 1400 and 2300 u MW peaks even though the MW of these peaks are slightly different from the 1200 u and 2400 u of hexamers and dodecamers. However, this attribution is justified by considering that at such long elution times the MW calibration curve is not perfectly reliable as the elution of heavy and structurally complex species could be affected by morphological factors. At this stage this inference remains a speculation needing more experimental work and suitable calibration standards. Interestingly, Figs. 4,5 show that the 600 u species are the most abundant and take into account for most of the reactor particle absorption hinting to the predominant formation of small oligomers, from dimers to tetramers, being trimers the most favored species in the investigated conditions.

In order to gain insights from the PSD and the concentration of the pyrene measured at the entrance of the reactor on the chemistry leading

Table 2
Conversion calculated from the PSD.

| $C_{Pirene}$, [ppm] | $T_{Reactor}$ [K] | Residence time [s] | Conversion [-] |
|---|---|---|---|
| 5.2 | 900 | 0.101 | 1.0E−05 |
| 5.2 | 1000 | 0.091 | 1.4E−04 |
| 5.2 | 1100 | 0.082 | 3.3E−04 |
| 47 | 1000 | 0.091 | 1.3E−04 |
| 47 | 1100 | 0.082 | 3.5E−04 |

the process of nucleation, some kinetics parameters reported in Table 2 have been retrieved. The conversion has been calculated both considering a spherical approximation and considering species with MW of 600 u in average over the mass of fed pyrene. In both cases the results were quite similar. A mean of the two values is reported in Table 2 and has been used for calculation. The absolute value of the particles formed is not reported, however it can be noted that the dependence of the particle formation on the pyrene concentration is not quadratic as expected hinting to a sticking mechanism. The dependence of particle formed on the pyrene concentration in the reactor can be retrieved. The conversion does not change with the pyrene concentration as in first order kinetic. Plotting the conversion against 1/T (Arrhenius plot) and kinetic constant assumes the form of a straight line, the gradient – i.e. the angular coefficient – corresponds to Ea/R. By applying this procedure, the activation energy estimated is 21,000 (±2000) Kcal/mol. This result suggests that the process is strongly dependent on the temperature which is the same evidence retrieved from PSD analysis.

To better study nucleation, the process has been considered divided in two steps: first the radical is formed and then the radical reacts with a stable molecule to form a stable dimer. Dimers are here intended as entities not belonging to gas-phase, formed by a chemically driven mechanism rather than by a physical sticking as that occurring in excimer formation [37,38] since physical dimers occurrence is generally not feasible at high temperatures. These dimers can be viewed as the first nucleus or the first particle (although the solid state feature generally attributed to particles is yet to be assessed for this structure). It is possible that the fluorescence spectra of the physical dimers and chemical dimers might be similar [7,39].

To form the radical from pyrene molecule it was not possible to adopt the unimolecular reactions, as no satisfying fitting of the results, regardless of the reaction rate adopted for the dimerization. The formation of pyrene radicals has been here hypothesized as a bimolecular reaction involving other stable species. Hereafter the two reactions:

$$A4 + M \Rightarrow A4 - + H + M \qquad (R1)$$

Table 3
Kinetic parameters of the hypothesized reactions. $A_0$ in mol cm$^3$ s$^{-1}$ – Ea in Kcal/mol and in Ev.

| | Estimated $A_0$ | Estimated Ea | |
|---|---|---|---|
| | | Kcal/mol | eV |
| **R1** | 1(±0.5)*E*+11 | 31,000 (±1500) | 1345 (±65) |
| **R2** | 2(±1)*E*+12 | 0 (±2500) | 0 (±108) |

$$A4 + A4- \Rightarrow DIM \quad (R2)$$

being A4 and A4- the pyrene and its radical and DIM the first condensed phase compound.

Collision frequency and activation energy for both reactions were retrieved to have the best fit for the experimental data (conversion) and are reported in Table 3.

The activation energy found for the radical formation is lower than the unimolecular case (101,000 Kcal/mol) but higher than the radical formation driven by H (45,000 Kcal/mol) or OH (45,000 Kcal/mol). In reaction (1) M is considered a stable species as nitrogen. Pre-exponential factors are similar to those found in literature for similar H-abstraction reactions, within the gas kinetic limit. Radical formation is a limiting step in the investigated conditions. After radical is formed its capability to form a dimer is quite high. In fact, the activation energy has been estimated to be close to 0. It was not possible to be more precise with the current measurements. These data suggest that the dimerization mechanism is driven by radicals. In previous works [1,2,11,22–24,40–42], this process has been already hypothesized using different models putting in evidence the presence of radicals on the particles; however this paper provides the first experimental evidence that starting from a PAH as pyrene, first a radical has to be formed and then has to be involved in the process, in order to justify the conversion rate of pyrene to nucleated particles in the investigated conditions. Also, the chemical-physical analysis has shown the oligomeric character of these particles that have lost the molecular features, hence they should not be longer considered in gas phase. The approximation used here of the two-step process is the simplest possible approach and the fit with experimental data was satisfying. The proposed pathways could still be an approximation of more complex processes but at this stage this would be speculative and needs more work.

## Conclusions

A specific experimental equipment has been set up in order to study the nucleation process of nanoparticles from the heating of molecules of PAH as pyrene into a 3.6-meter tubular flow reactor heated up with ceramic heaters. PSD of particles at the exit of the reactor were measured by DMA. A controlled flow of pre-heated argon has been employed to sublimate pyrene placed in a quartz saturator and conveyed into the entrance of the reactor.

Different PSD at the exit of the reactor, measured by using a DMA with a size range 0.6–28 nm, have been found by varying reactor (800 to 1100 K) and quartz saturator temperature, i.e., varying pyrene concentration in the reactor. Particle formation was found sensitive to the temperature. In particular, the formation rate was higher as the temperature in the reactor was higher, suggesting the intervention of some chemical-driven pathway from the formation of the first condensed-phase species. Particles sampled in ethanol by means of a bubbler at the reactor exit were analyzed with SEC and UV-Visible absorption. The smallest species in condensed phase appeared to be species that have lost molecular-like absorption features and present molecular weight from 400 to about 800 u, peaked around 600 u, consistently with a pyrene oligomerization process.

A two-step mechanism for the formation of pyrene oligomers as dimers was hypothesized. First the radical is formed by collision of pyrene with other stable molecules (nitrogen), then the radical formed reacts with stable pyrene to form a dimer. The first stage was found to be very slow and thus the limiting one in the investigated conditions.

## Declaration of Competing Interest

None.

## Acknowledgments

The authors would like to thank Dr. Anna Ciajolo for her invaluable advices and inspiring discussion during the studies and writing process of this research.

## Supplementary materials

Supplementary material associated with this article can be found, in the online version, at doi:10.1016/j.proci.2020.06.367.

## References

[1] A. D'Anna, *Proc. Combust. Inst.* 32 (2009) 593–613.
[2] H. Wang, *Proc. Combust. Inst.* 33 (2011) 41–67.
[3] P. Desgroux, A. Faccinetto, X. Mercier, T. Mouton, D.A. Karkar, El Bakali, *Combust. Flame* 184 (2017) 153–166.
[4] M. Sirignano, D. Bartos, M. Conturso, M. Dunn, A. D'Anna, A.R. Masri, *Combust. Flame* 176 (2017) 299–308.

[5] M. Sirignano, A. Collina, M. Commodo, P. Minutolo, A. D'Anna, *Combust. Flame* 159 (2012) 1663–1669.
[6] P. Minutolo, G. Gambi, A. D'Alessio, A. D'Anna, *Combust. Sci. Tech.* 101 (1–6) (1994) 311–325.
[7] F. Ossler, T. Metz, M. Alden, *Appl. Phys. B* 478 (2001) 465–478.
[8] H. Bladh, N.-.E. Olofsson, T. Mouton, et al., *Proc. Combust. Inst.* 35 (2015) 1843–1850.
[9] B. Apicella, P. Pré, M. Alfè, et al., *Proc. Combust. Inst.* 35 (2015) 1895–1902.
[10] G. De Falco, M. Commodo, C. Bonavolontà, G.P. Pepe, P. Minutolo, A. D'Anna, *Combust. Flame* 161 (12) (2014) 3201–3210.
[11] F. Schulz, M. Commodo, K. Kaiser, et al., *Proc. Combust. Inst.* 37 (1) (2019) 885–892.
[12] M. Commodo, G. De Falco, A. Bruno, C. Borriello, P. Minutolo, A. D'Anna, *Combust. Flame* 162 (10) (2015) 3854–3863.
[13] M. Thierley, H.H. Grotheer, M. Aigner, et al., *Proc. Combust. Inst.* 31 (2007) 639–647.
[14] J. Happold, H.H. Grotheer, M. Aigner, *Rapid Commun. Mass Spectrom.* 21 (7) (2007) 1247–1254 An International Journal Devoted to the Rapid Dissemination of Up-to-the-Minute Research in Mass Spectrometry.
[15] Q. Mao, A.C.T. van Duin, K.H. Luo, *Carbon N Y* 121 (2017) 380–388.
[16] C.A. Schuetz, M. Frenklach, *Proc. Combust. Inst.* 29 (2002) 2307–2314.
[17] J.D. Herdman, J.H. Miller, *J. Phys. Chem. A* 112 (2008) 6249–6256.
[18] S.H. Chung, A. Violi, *J. Chem. Phys.* 132 (2010) 174502 Article.
[19] T.S. Totton, A.J. Misquitta, M. Kraft, *Chem. Theory Comp.* 6 (2010) 683–695.
[20] S. Iavarone, L. Pascazio, M. Sirignano, et al., *Combust. Theor. Model.* 21 (2017) 49–61.
[21] L. Pascazio, M. Sirignano, A. D'Anna, *Combust. Flame* 185 (2017) 53–62.
[22] A. D'Anna, A. Violi, A. D'Alessio, A.F. Sarofim, *Combust. Flame* 127 (2001) 1995–2003.
[23] M. Thomson, T. Mitra, *Science* 361 (6406) (2018) 978–979.
[24] K.O. Johansson, M.P. Head-Gordon, P.E. Schrader, K.R. Wilson, H.A. Michelsen, *Science* 361 (6406) (2018) 997–1000.
[25] B. Shukla, M. Koshi, *PCCP* 12 (10) (2010) 2427–2437.
[26] B. Shukla, A. Susa, A. Miyoshi, M. Koshi, *J. Phys. Chem. A* 111 (34) (2007) 8308–8324.
[27] B. Shukla, A. Susa, A. Miyoshi, M. Koshi, *J. Phys. Chem. A* 112 (11) (2008) 2362–2369.
[28] B. Shukla, M. Koshi, *Combust. Flame* 158 (2) (2011) 369–375.
[29] A. Ergut, S. Granata, J. Jordan, et al., *Combust. Flame* 144 (4) (2006) 757–772.
[30] A. Ergut, Y.A. Levendis, H. Richter, J.B. Howard, J. Carlson, *Combust. Flame* 151 (1–2) (2007) 173–195.
[31] K. Ono, Y. Matsukawa, K. Dewa, et al., *Combust. Flame* 162 (6) (2015) 2670–2678.
[32] A.F. Sarofim, J.P. Longwell, M.J. Wornat, J. Mukherje, Springer, Berlin, 1994, p. 485.
[33] C. Russo, B. Apicella, A. Ciajolo, *Sci. Rep.* 9 (1) (2019) 1–8.
[34] C. Russo, F. Stanzione, A. Ciajolo, A. Tregrossi, *Proc. Combust. Inst.* 34 (2) (2013) 3661–3668.
[35] A.D. Abid, E.D. Tolmachoff, D.J. Phares, H. Wang, Y. Liu, A. Laskin, *Proc. Combust. Inst.* 32 (1) (2009) 681–688.
[36] A. D'Alessio, A.C. Barone, R. Cau, A. D'Anna, *Proc. Combust. Inst.* 30 (2005) 2595–2603.
[37] J.B. Birks, *Photophysics of Aromatic Molecules*, 1st edition, Wiley-Interscience, London, 1970.
[38] J.B. Birks, L.G. Christophorou, *Nature* 194 (1962) 442–444.
[39] F. Ossler, T. Metz, M. Aldén, *Appl. Phys. B* 72 (4) (2001) 479–489.
[40] J.W. Martin, D. Hou, A. Menon, et al., *J. Phys. Chem. C* 123 (2019) 26673–26682.
[41] M.R. Kholghy, G.A. Kelesidis, S.E. Pratsinis, *Phys. Chem. Chem. Phys.* 20 (2018) 10926–10938.
[42] H. Yuan, W. Kong, F. Liu, D. Chen, *Chem. Eng. Sci.* 195 (2019) 748–757.